Thunderstorms and Total Lightning Characteristics Causing Heavy Precipitation in Japan : A Case Study

Debrupa Mondal[1], Yasuhide Hobara[1,2], Hiroshi Kikuchi[2], Jeff Lapierre[3]

[1]Graduate School of Informatics and Engineering, University of Electro-Communications, 1-5-1, Chofugaoka, Chofu-shi, Tokyo 182-8585, Japan
E-mail: debrupamondaljam@gmail.com

[2]Center for Space Science and Radio Engineering, University of Electro-Communications

[3]Earth Networks, Germantown, MD 20874, USA

Abstract

We have analyzed an isolated, multicellular thunderstorm event with heavy precipitation (~100 mm/h) that occurred in Saitama, Japan. The X-band multi-parameter radar-derived 3D volume scan and ground-based total lightning data provide detailed spatio-temporal dependences of precipitation cores in different altitudes and associated different types of lightning. We found the development of high altitude (~7-10 km) precipitation core shows a high correlation with the in-cloud lightning rate and the peak of IC lightning occurred 5-10 min prior to subsequent heavy precipitation on the ground. Again, ground precipitation shows a higher correlation with -CG than +CG without significant time lag. Therefore, monitoring total lightning activity during thunderstorms can be useful for nowcasting and short-time prediction of ground precipitation volume.

1. Introduction

The frequency of natural disasters from extreme weather events (heavy precipitation (50mm/h) causing flash floods, storm surges, hurricanes, etc.) is increasing worldwide, including in Japan, due to the faster surface temperature rise (~0.5°C) than the global average (~0.3°C), and scientists predict this long-term trend will continue steadily or may increase [1]. To mitigate the huge destruction associated with such kinds of events, it is important to predict them sufficiently before their occurrence. Many studies showed the Total Lightning (TL) behavior (both In-Cloud (IC) and Cloud-to-Ground (CG)) and its correlation with severe weather such as hail and wind gusts associated with ThunderStorms (TS), tornadoes etc [2,3]. Also, different research groups have investigated spatial distribution trends [4,5], and temporal dependencies [6,7] between lightning and heavy precipitation and found that lightning can act as a precursory parameter of heavy precipitation. Sun *et al* [4], Wang and Liao [5] showed that positive CG flashes occur at the center of the precipitation core and are more in phase with high-level radar reflectivity. Gungle and Kridar [7] showed a linear relationship between the ground Precipitation Volume (PV) and the number of CG flashes and a variable time lag of 5-20 minutes (CG increases before precipitation increases) observed for these warm season storms in Florida.

In the developing stage of a TS, as a result of the strong updraft, IC pulses are produced in the initial stage of cloud electrification and CG flashes are more common in the mature stage of the storm. So, compared to less CG (~30%), a very large number of IC (~70%) as well as TL improves the accuracy of forecasting and warning time [8, 9].

Few research works have been made for the TS events in Japan with heavy precipitation and TL. Ogawa *et al.* (2018) showed a strong positive correlation between the time series of lightning stroke rate from Japanese Total Lightning Network data and ground PV using XRAIN data along with other meteorological parameters but no major time lag between these two was observed [10].

In this paper we have analyzed the overall picture of the development of TS clouds and precipitation cores associated with TSs that produce heavy precipitation (max >100 mm/h) by using TL data and full-volume scan high-speed weather radar data. We have also examined a time lag between the occurrence of lightning activity and

Table 1. XRAIN data specifications

Collected data	Precipitation (mm/h)
Time resolution	1 min
Spatial resolution	250 m
Precipitation resolution	0.1 mm/h
Minimum value	0.1 mm/h
Maximum value	409.0 mm/h

maximum precipitation which could be used for forecast/ nowcast purposes for short-duration extreme rainfall events.

2. Data Collection

2.1 eXtended RAdar Information Network (XRAIN)

In this study we have used precipitation data from the Ministry of Land, Infrastructure, Transport, and Tourism's eXtended RAdar Information Network. The network is composed of 26 C-band radars and 39 X-band multiparameter (X-MP) radars which cover most parts of Japan around 14 major cities [11]. The full volume scan data produced by these X-MP radar scanning, are collected to visualize the precipitation core development at a higher altitude in 5-min time resolution. Twelve elevation angles are scanned to produce the 3D data ranging from 0° to 20°. X-band and C-band radar-derived high-resolution (temporal resolution of 1 min, spatial resolution of 250 m) composite ground rainfall intensity data [mm/h] is also collected from XRAIN. The ground rainfall data specifications are summarized in Table 1.

2.2 Japanese Total Lightning Network (JTLN)

TL data associated with the event is collected from JTLN which consists of 11 Earth Networks Total Lightning Sensors (Figure 1) over Japan (data set in 2017, currently 16 stations nationwide) deployed by the University of Electro-Communications and jointly operated with Earth Networks. These sensors can detect lightning pulses in a wide frequency range, ranging from 1 Hz to 12 MHz i.e., extreme low frequency to high frequency range with a spatial resolution of 500 m. TL parameters such as types of lightning (IC and CG), time of occurrence (UT), location (latitude-longitude), and lightning polarity are collected for each lightning discharge.

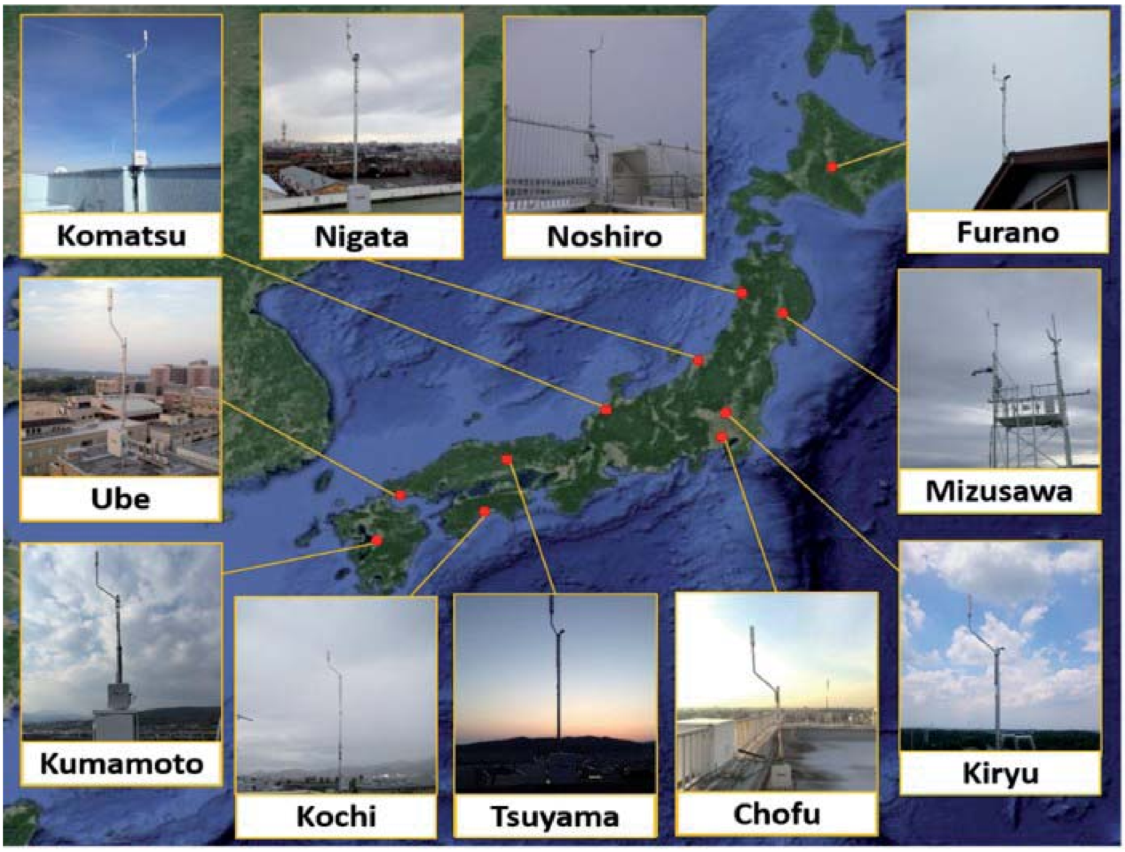

Figure 1. JTLN sensor distribution over Japan.

3. Results

In this paper, the preliminary results from the data analysis of high-resolution 3D volume scan precipitation data and TL activity have been presented. An isolated TS event with heavy precipitation, that occurred in Saitama prefecture and caused flooding of Yanase river on August 30, 2017, is analyzed in detail. During this TS event, the maximum precipitation rate of >100 mm/h (instantaneous value which represents 100 mm of rain would fall in 1 h if the rain rate remained constant) was observed by XRAIN. Depending on the different developmental stages at a particular time, different cells of a smaller spatial scale are considered (multicell TSs).

3.1 Spatio-temporal distribution

From every 5-min full volume scan data of Shinyoko radar (35.5125° E, 139.5994° N), Constant Altitude Plan Position Indicator (CAPPI) plots were produced and

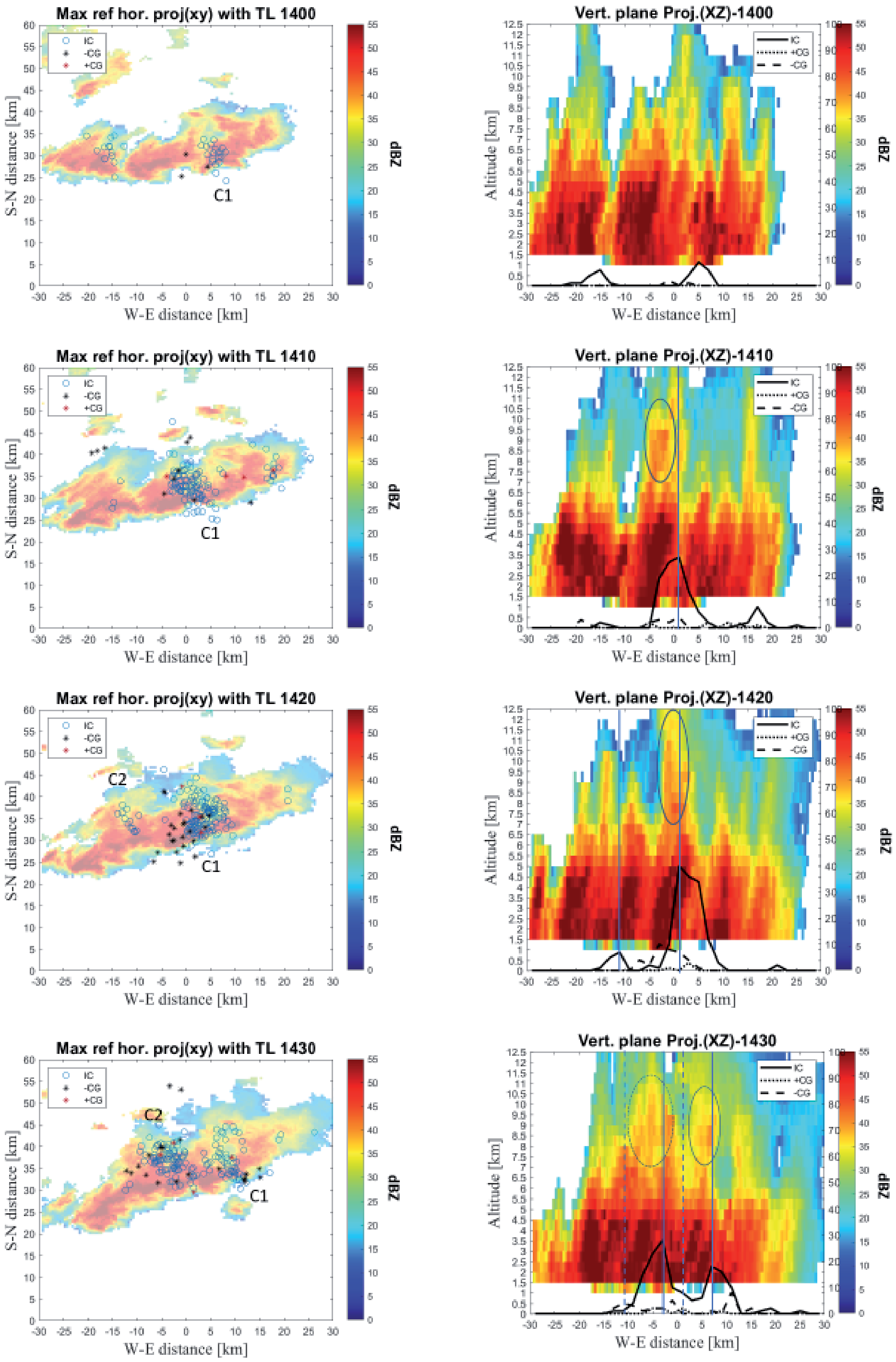

Figure 2. Maximum radar reflectivity projections on horizontal (left panels) and vertical planes (right panels) along with the lightning distributions for the first thirty minutes of the storm starting from 1400 JST.

a smaller area of analysis was selected depending on precipitation cell location. For a detailed analysis with TL distribution, we took maximum radar reflectivity projection both on horizontal (SN-WE) and vertical planes (WE-Altitude) for the selected range. The left panels of each time step in Figure 2 show the maximum radar reflectivity projection on the horizontal plane (for altitude range 0-12 km) with the spatial distribution of IC (blue circle), +CG (red asterisk), -CG (black asterisk) for the first thirty minutes of the TS. The horizontal axis represents the WE distance [km] from the radar location and the vertical axis represents the SN distance [km] from the radar (the radar is located at (0,0)). The right panels of each time step in Figure 2 show the maximum radar reflectivity projection on the vertical (WE-Altitude) plane (for SN range 0-60 km). The lightning data i.e. IC (black solid line), +CG (black dotted line), -CG (black dashed line) flash rate per 5 min for every 2 km of WE range and the SN range of 0-60 km. Observing the distribution of TL, we consider two precipitation cells formation and dissipation during the life cycle of the TS.

The first cell (C1 in Figure 2) started evolving around 14:00 JST (Japan Standard Time) within the 5 km east

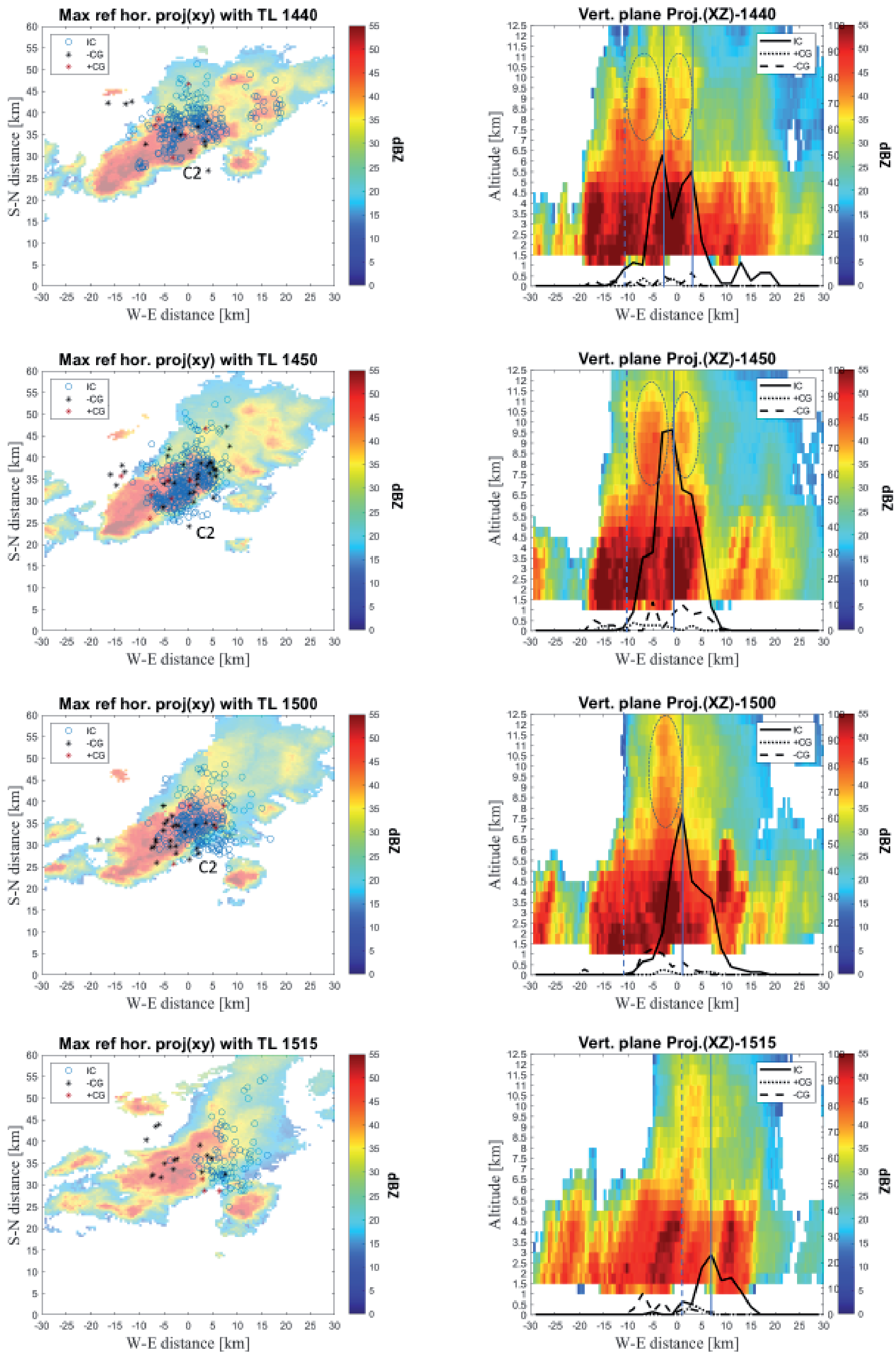

Figure 3. Maximum radar reflectivity projections on horizontal (left panels) and vertical planes (right panels) along with the lightning distribution for the remaining stages of the thunderstorm's life cycle.

of radar location. IC pulses gradually increased from 20 pulses per 5 min at 14:00 JST to 135 pulses per 5 min at 14:20 JST. TS cloud also started developing above 7 km altitude and with an IC lightning jump around 14:10 JST (a rapid increase from 19 pulses to 92 pulses/5 min), a strong core formation (blue circle in Figure 2) was observed at higher altitude (>7 km). This strong core evolved to max height (~12 km) around 14:20 JST when the IC count (135 pulses/5 min) was maximum. Around 14:20 JST few dispersed -CG strokes were observed a bit westward of IC concentration. IC pulses started decreasing gradually after this and started shifting eastward. The precipitation core at high altitudes also started diminishing. Around 14:20 JST, IC pulses also started increasing nearly 10 km west of the radar location and the peak gradually shifted eastward, which is considered as the second cell (C2 in Figure 2 and Figure 3). Simultaneously, TS cells also started evolving above 7 km altitude.

Figure 3 shows the maximum radar reflectivity projections on horizontal (left panels) and vertical planes (right panels) same as in Figure 2 but for the remaining stages of the TS's life cycle. Around 14:40 JST IC distribution is seen to be concentrated in two adjacent locations (2 peaks with consecutive 48 and 42 pulses/5 min in a 2 km range) and two relevant clear precipitation cores (blue dashed circle in Figure 2) were also identifiable in higher altitudes which belongs to second cell i.e. C2. Since C1 already started diminishing around 14:30, only C2 is shown in Figure 3.

After attaining the peak IC at 14:50, these two cores merged and sustained till 15:00 and then gradually started diminishing. IC flash rate also decreased and the peak of IC shifted eastward. The maximum CG (Positive CG + Negative CG) rate was observed around 14:55 (not shown in the figure).

For both the cells of this heavy precipitation event, precipitation cores at higher altitudes (above 7 km) started evolving around 2-4 km west from the peak IC lightning location and gradually migrated towards the peak location. In Figure 2 and Figure 3, the dashed vertical line shows the previous IC peak location and the solid vertical line shows the current IC peak location which also shifts a bit eastward with time. The developed cores faded with the decrease in IC pulses. CG pulses are found to be concentrated in the precipitation core region just before maximum ground precipitation.

Next, we have analyzed the temporal evolution of high altitude and ground PV as well as the TL, IC, and both +CG and -CG rates. Depending on the lightning distribution (or, lightning core area), we selected the area (range of the cell in SN and WE direction) of both the cells with time and calculated the above-mentioned parameters. Figure 4(a) shows the time series of high altitude (7-10 km) PV (solid blue line) and IC (black dashed line) and CG (red dashed line) pulse rates per 5 min for the 2nd cell (C2). The peak of IC (around 350 pulses/5 min) and PV around 7-10 km occurred simultaneously at 14:50 JST, whereas the ground PV peak (blue solid) occurred around 10 min later than the IC peak (black dashed) as shown in Figure 4(b). The peak CG (53 pulses/5 min, red dotted line) was observed 5 min before the peak of the ground precipitation. A similar time delay between rapid IC increase and ground precipitation is also observed for cell 1.

3.2 Correlation between lightning and precipitation

We have carried out a cross-correlation analysis between different lightning rates and PV (normalized cross-correlation between IC rate and high-altitude PV, IC rate and ground PV, CG rate and ground PV for the same time series) during the entire storm period. After cross-correlation, and considering the resultant time lag, the maximum correlation coefficients have been calculated. Figure 5(a) shows the cross-correlation function of IC vs high-altitude PV for the second cell and Figure 5(b) shows the scatter plot and maximum correlation coefficient of the same. Higher altitude PV and IC rate showed a high correlation (correlation coefficient, R=0.95) and no time lag. Similarly, for cell 1, max cross correlation between IC and (7-10km)

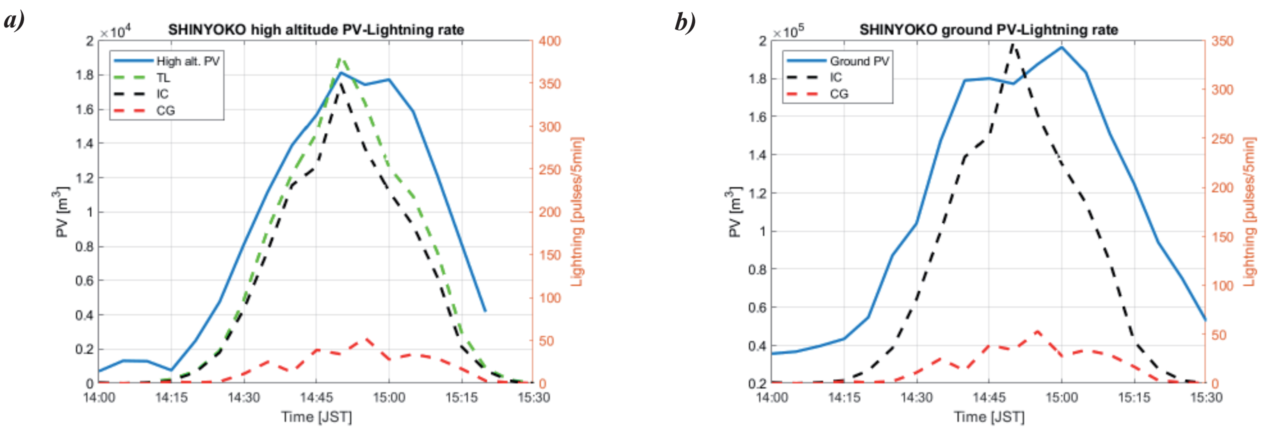

Figure 4. Temporal evolutions of (a) high-altitude PV and TL, IC, CG pulse rates, and (b) ground PV and IC, CG pulse rates.

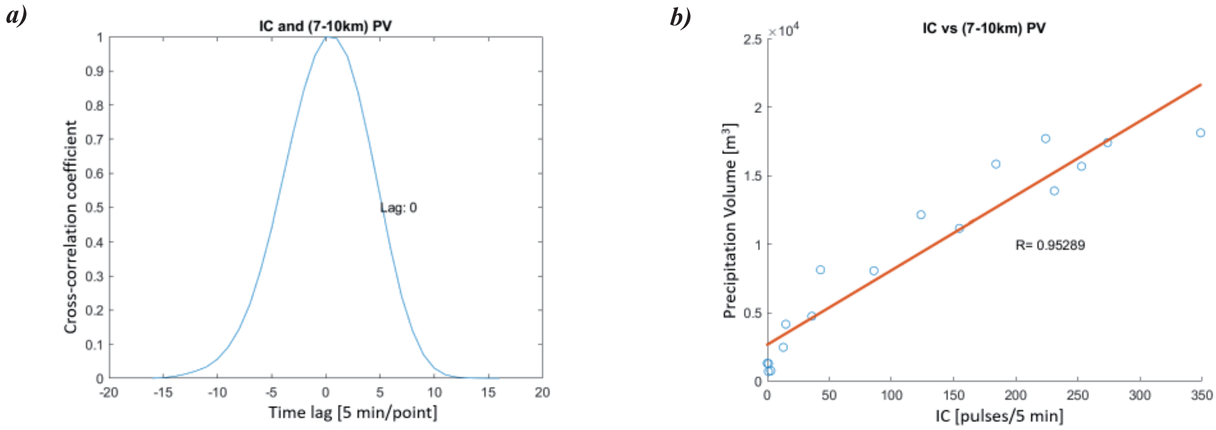

Figure 5. (a) Cross-correlation coefficient between IC and high-altitude PV for cell 2, and (b) relationship between IC [pulses/5min] and high-altitude PV.

PV is observed to be 0.96 (not in figure). These R-values, calculated for individual cells (selected according to the TL distribution) of a smaller spatial scale are significantly higher than the correlation coefficient (0.84) calculated for IC (as well as TL) and ground PV, considering the entire storm in the previous study [10]. Moreover, a positive lag (lag =1 i.e., time lag = 5min) between ground PV and IC rate is also observed which indicates IC pulses are 5 ~ 10 min ahead of ground PV for the entire TS activity. Figure 6(a) represents the cross-correlation function of negative CG vs ground PV and Figure 6(b) shows the scatter plot and maximum correlation coefficient for the same. The ground PV is observed to be more correlated with -CG (R=0.88) than +CG (R=0.75, and the time lag between them is shorter than 5 min. Again, this correlation coefficient value is also much higher than the previous study (for CG and ground rainfall, R = 0.40).

4. Discussion

Yuan and Qie [12] showed a relatively stable relationship and high correlation (>0.7) between ice-phase precipitation (7-11 km) and lightning frequency. Though for the complete storm system, the ground precipitation correlates more with TL [10], the present study showed for individual cells of the same storm system, higher altitude precipitation (7-10 km) correlates more with IC. Instead of considering the entire storm, consideration of a smaller spatial scale (cell scale) and higher altitude precipitation results in significant improvement in the cross-correlation (from 0.84 to 0.95). Rapid intensification of the core at higher altitudes appears with more IC occurrence which indicates greater charge separation, thus strong updraft causing more ice particle collisions during the developing stage of a cell. Liu *et al* [8] showed continuous tracking of TL data, especially IC lightning enables tracking and prediction of different properties of high-impact weather events. For this particular event, consideration of the total storm scale resulted in only 2 min lead time [10], whilst we showed that individually for both the cells, the peak of IC (or, IC lightning jump) occurs nearly 5~10 min earlier than peak ground PV which may be used as a precursory parameter for short-term prediction of maximum ground rainfall. Besides the multicellular nature, we need to consider the correlation of merging-separation between the cells with lightning distribution in the TS life cycle and thus further analysis with more events is required.

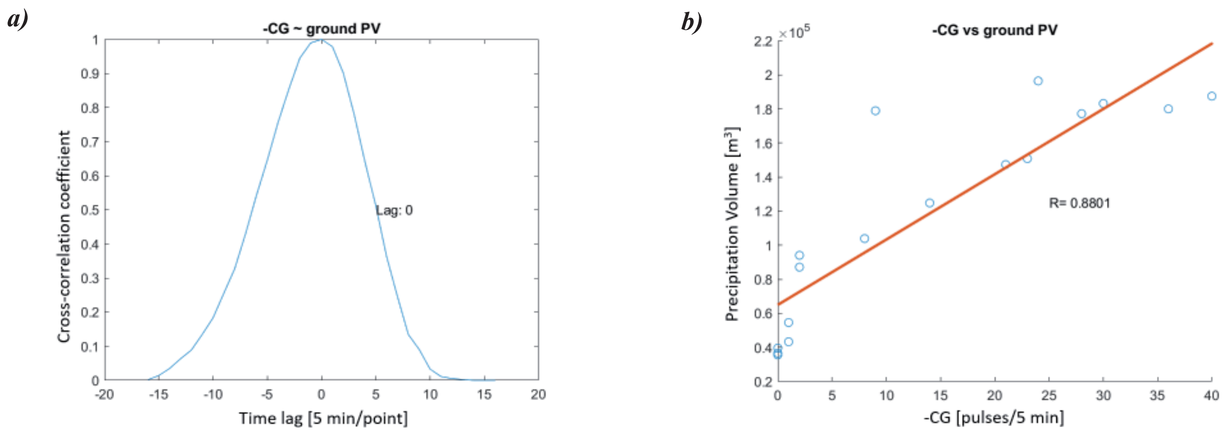

Figure 6. (a) Cross-correlation coefficient between -CG and ground PV for cell 2, and (b) relationship between CG [pulses/5min] and ground PV.

5. Acknowledgments

We acknowledge the support from the Ministry of Education, Culture, Sports, Science, and Technology (AiQuSci Scholarship). The authors are grateful to the Ministry of Land, Infrastructure, Transport and Tourism for providing XRAIN data and also to the KDDI foundation for supporting partially this research project. The authors also thank P. Le Floch and E. DiGangi of EN, Tada Farm, Noshiro City Children's Center, Niigata Science Museum, NAOJ Mizusawa, JAIST, Gunma Univ., Rissho Univ., ISEE (Nagoya Univ.), NIT Tsuyama College, Kochi Univ., Ama town, Yamaguchi Univ., Tokai Univ. for their help JTLN observations in Japan.

6. References

1. Nayak, K. Dairaku, I. Takayabu, A Suzuki-Parker, N. N. Ishizaki, "Extreme Precipitation Linked to Temperature Over Japan: Current Evaluation and Projected Changes With Multi-model Ensemble Downscaling," *Climate Dynamics*, **51**, 2018, pp. 4385–4401.

2. Pineda, J. Bech, T. Rigo, J. Montanyà, "A Mediterranean Nocturnal Heavy Rainfall and Tornadic Event. Part II: Total Lightning Analysis," *Atmospheric Research*, **100**, 2011, pp. 638–648.

3. Farnell, T. Rigo, N. Pineda, "Lightning Jump as A Nowcast Predictor: Application to Severe Weather Events In Catalonia," *Atmospheric Research*, **183**, 2017, pp. 130–141.

4. Sun, J. Chai, L. Leng, G. Xu, "Analysis of Lightning and Precipitation Activities in Three Severe Convective Events Based on Doppler Radar and Microwave Radiometer over the Central China Region," *Atmosphere*, **10**(6), 2019, p. 298

5.Y. Wang, S.A. Liao, "Lightning, Radar Reflectivity, Infrared Brightness Temperature, and Surface Rainfall During The 2–4 July 2004 Severe Convective System Over Taiwan Area," *Journal of Geophysical Research*, **111**, 2006, D05206.

6. Farnell, T. Rigo, "The Lightning Jump Algorithm for Nowcasting Convective Rainfall in Catalonia," *Atmosphere*, **11**(4), 2020, p. 397

7. Gungle, E. P. Krider, "Cloud-to-ground Lightning and Surface Rainfall in Warm-season Florida Thunderstorms," *Journal of Geophysical Research: Atmospheres,* **111**, 2006, D19203

8. Liu, C. Sloop, S. Heckman, "Application of Lightning in Predicting High Impact Weather," OBS/IMO/TECO-2014

9. A. Rakov and M. A. Uman, "*Lightning: Physics and Effects*", Cambridge: Cambridge University Press, 2003

10. Ogawa, Y. Hobara, H. Iwasaki, S. Heckman, M. Stock, "Statistical Study of The Relationship Between Total Lightning and Heavy Rainfall," 16th International Conference on Atmospheric Electricity, Nara, Japan, 2018

11. T. Maesaka, "Operational Rainfall Estimation by X-band MP Radar Network in MLIT, Japan," Environmental Science, September, 2011

12. T Yuan, X. S. Qie, "Study on Lightning Activity and Precipitation Characteristics Before and After the Onset of The South China Sea Summer Monsoon," *Journal of Geophysical Research*, **113**, 2008, D14101.